Activity Monitoring of Functional OprM Using a Biomimetic Microfluidic Device

Wei Wang, Laura Monlezun, Martin Picard, Philippe Benas, Olivier Français, Isabelle Broutin, Bruno Le Pioufle

Activity Monitoring of Functional OprM Using a Biomimetic Microfluidic Device

Wei Wang, [§a] *Laura Monlezun*, [§b] *Martin Picard*, [b] *Philippe Benas*, [b] *Olivier Français*, [a] *Isabelle Broutin* ‡*[b], *Bruno Le Pioufle*, ‡*[a]

[a] SATIE, UMR 8029 CNRS, Ecole Normale Supérieure de Cachan, 61 Avenue du Président Wilson, 94235 Cachan cedex, France. E-mail: bruno.lepioufle@satie.ens-cachan.fr

[b] Laboratoire de Cristallographie et RMN Biologiques, Université Paris Descartes, Sorbonne Paris Cité, UMR 8015 CNRS, Faculté des Sciences Pharmaceutiques et Biologiques, 4 Avenue de l'Observatoire, 75270 Paris cedex 06, France. E-mail: isabelle.broutin@parisdescartes.fr

[§] Wei Wang fabricated the microfluidic devices, performed BLM formation, ion channel insertion, electrical monitoring and signal processing of its activities. Laura Monlezun prepared all the membrane protein samples used in that study.

‡ Co-corresponding authors.

ABSTRACT:

This paper describes the fabrication and use of a biomimetic microfluidic device for the monitoring of a functional porin reconstituted within miniaturized suspended artificial bilayer lipid membrane (BLM). Such a microfluidic device allows for 1) fluidic and electrical access to both sides of the BLM, 2) reproducible membrane protein insertion and long-term electrical monitoring of its conductance (Gi), thanks to the miniaturization of the BLM. We demonstrate here for the first time the feasibility to insert a large trans-membrane protein through its β-barrel, and monitor its functional activity during more than 1 hour (limited by buffer evaporation). In this paper, we specifically used our device for the monitoring of OprM, a bacterial efflux channel involved in the multidrug resistance of the bacteria Pseudomonas aeruginosa. Sub-steps of the OprM channel conductance were detected during the electrical recordings within our device, which might be due to oscillations between several structural conformations (sub-states) adopted by the protein, as part of its opening mechanism. This work is a first step towards the establishing of a genuine platform dedicated to the investigation of bacterial proteins under reconstituted conditions, a very promising tool for the screening of new inhibitors against bacterial channels involved in drug resistance.

1. Introduction

The study of the conductance of bacterial ion channels is highly important for the research in pharmacology as they are crucial in active efflux, one of the main mechanisms involved in the resistance of bacteria to antibiotics.[1] Two different classes of porins exist respectively responsible for the influx and the efflux across the outer membrane of Gram negative

bacteria.[2-4] Even though the first porin has been described in 1970 and our knowledge concerning this family of proteins continually progress since that time, several questions still remain open regarding their function, especially on their opening mechanism.

In the case of the Gram-negative bacteria *Pseudomonas aeruginosa*, four different efflux pumps have been characterized. One of them is the OprM/MexA/MexB complex which is reversibly assembled to allow for the transport across the two membranes of the bacteria. OprM, a porin part of the OMF (Outer Membrane Factor) family, is inserted into the external membrane (Fig. 1a).

The crystallographic structure of OprM has already been presented with various resolutions.[5,6] It has been proposed that the opening of OprM could be due to a twist movement, equivalent to that of a photographic diaphragm,[7] combined with an extension movement, involving the cooperative reorganization of key residues at both ends (Fig. 1b,c).[6]

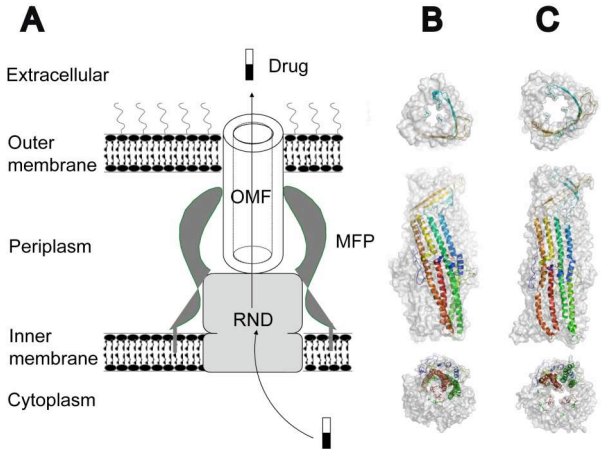

Fig. 1 (A) **S**chematic representation of an efflux pump from the type I transporter family. (B) Closed and (C) open states of the OprM porin.

The activity of porins and channels is classically addressed by measuring the change of membrane conductance after insertion of proteins in an artificial bilayer separating two compartments.[8] Micro-technologies have been developed to miniaturize the aperture permitting the reconstruction of artificial bilayer lipid membrane (BLM), as it benefits to its

stability.[9-13] In that case the artificial BLM can be connected to a microfluidic structure.[14] The functionality of such miniaturized biosensors was proved previously by using model ion channel peptides (gramidicin or alamethicin) and α-hemolysin.[12,15,16] Nevertheless, results obtained with these model peptides can not illustrate the difficulties that can be encountered when investigating actual porin proteins. Indeed, the insertion of OprM through its β-barrel, which represents only a third of the protein length, is totally different from the extremely stable insertion of α-hemolysin with its large stabilizing rubber rings.

We demonstrate in this paper through repeatable conductance measurements that single native OprM channel insertion can be achieved reproducibly by using our microfluidic device. Moreover the microsized dimension of the artificial bilayer allows long-term monitoring of the conductance of OprM.

After the initial insertion of OprM, correlated with a significant step in term of conductance increase, fluctuation of the conductance between several sub-steps could be clearly identified. These fluctuations might be due to oscillations between several conformations of the protein, presumably of its internal helix bundles, which lead to variations of the conductance.

This work contributes to a better understanding of OprM activity, which is an important step prior to the next challenge that will be the screening of chemical compounds for the discovery of new inhibitors of the bacterial efflux pumps.

2. Experiment section

2.1. Design and Fabrication

The structure of the microfluidic device used in this work, which is inspired from the microarray design described before,[12] is briefly summarized hereafter. The chip is based on two bonded PMMA layers separated by a parylene film. A picture of the device within the experimental setup is shown in Fig. 2a, while a schematic view is represented in Fig. 2b.

The top PMMA substrate includes a chamber for buffer reservoir and access for the recording electrode as shown in Fig. 2c. A recess in this top substrate allows the alignment of the self-standing parylene film (Fig. 2a). The bottom PMMA substrate has a fluidic channel for liquid injection (lipid and buffer), of which top and bottom faces are defined by the parylene film and a microscope cover glass, respectively (thickness = 170 µm). Micrometer-sized apertures have been etched in the parylene film enabling lipid bilayer formation (Fig. 2c). Fabrication process of the microfluidic chip relies on three main steps described as follows:

Firstly, parylene film is deposited on a single-crystal silicon substrate by chemical vapor deposition technique at a thickness of 10 µm. Holes are then etched in the film by RIE oxygen plasma using an aluminum mask as protective layer. After removing the aluminum, the parylene film (with microapertures from 20 to 100 µm diameter) is peeled off from the silicon substrate using tweezers. The thickness of parylene film is optimized by combining the considerations of easy peeling and BLM formation.

Secondly, the PMMA substrates are machined using simple drilling and milling techniques to obtain the bottom plate including the fluidic channel (W = 2 mm, H = 0.5 mm, L = 25 mm) and the top plate including the chamber (Ø = 4 mm, H = 1.5 mm), and a recess for the alignment with parylene film (8.1 mm×8.1 mm×0.1 mm).

The third step concerns the full packaging of the device. UV sensible adhesive layer (NOA 73, Norland products, NJ USA) was used to bond the parylene film between the two PMMA substrates. A microscope cover glass was finally glued to close the bottom channel.

Several prototypes with varying diameter apertures were fabricated. Final choice of the aperture diameter depends on the stability and sealing resistance of BLM. In the case of the recordings presented in this paper, the diameter was set to 45 µm.

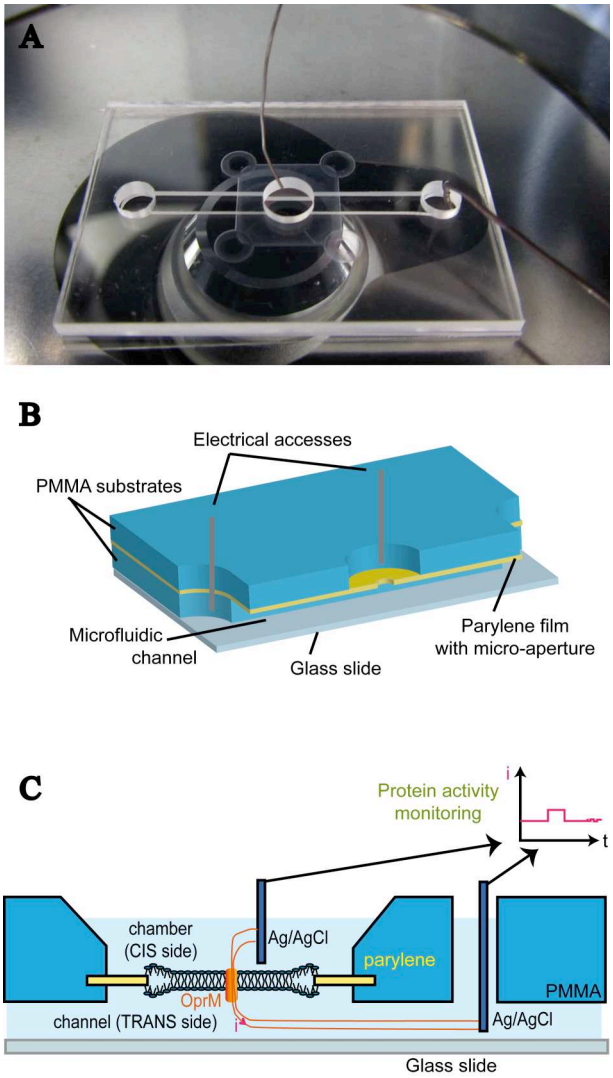

Fig. 2 Microfluidic biomimetic device: (A) view of the microfluidic device on the microscope stage, (B) scheme of the structure of the device. A thin film of parylene previously micromachined is sandwiched between two PMMA plates in which are machined the *CIS* chamber and *TRANS* fluidic access and channel. (C) Cross section: an ion channel reconstituted in BLM within the microfluidic chip is electrically monitored by using a patch clamp amplifier.

2.2. Reagents

For the lipid solution, 25 mg of 1,2-diphytanoyl-sn-glycero-3-phosphocholine (DPhPC) or L-α-phosphatidylcholine (PC) (Avanti Polar Lipids, U.S.A.) dissolved in 1 mL or 500 µL of mixed solvents of n-decane (20%, 50% or 100% in v/v) and 1-hexanol (80%, 50% or 0% in v/v) was used. For the buffer solution of the experiments performed with Na^+ ions, 50 mM

sodium phosphate, 100 mM NaCl, 5% (v/v) Glycerol at pH = 7.5 was used. For the experiments performed with K^+ ions, 10 mM 4-(2-hydroxyethyl)-1-piperazineethanesulfonic acid (HEPES), 5% (v/v) Glycerol at pH 7.5, and either 150 mM KCl or 1 M KCl were used as buffer. Stock solutions of OprM were diluted down to 5 µg/ml in the respective buffers complemented with 0.45% (w/v) Octyl-β-d-glucopyranoside (βOG) before use.

2.3. Expression, Purification and Preparation of the Protein

Vector pBAD33-GFPuv was used to heterologously express and purify OprM with a C-terminal 6-histidine tag, from the *Escherichia coli* C43-DE3 strain as described previously.[6] Cultures were performed at 30°C in Lysogeny broth (LB) medium containing 25 µg/ml chloramphenicol, induced at A_{600} = 0.8 by the addition of 0,02% (w/v) L-arabinose and grown for 2 h before centrifugation. The cell pellet was resuspended in Tris-HCl 20 mM pH 8.0. Cells were broken by a French pressure cell at 69 MPa (*i.e.* 10.000 psi) and then centrifuged twice at 8.500 g to remove the inclusions bodies and unbroken cells. The soluble fraction was applied on a sucrose step gradient (0.5 and 1.5 M) and then centrifuged for 3 h at 200.000 g, 4°C. The pellet, corresponding to the outer membrane fraction, was resuspended in a solution containing 20 mM Tris-HCl pH 8.0, 10% glycerol (v/v), 2% βOG (w/v) (Anatrace), then stirred overnight at 23°C. The solubilized membrane proteins were recovered by centrifugation for 30 min at 50.000 g and further loaded onto a Ni-NTA resin column pre-equilibrated in 20 mM Tris-HCl pH 8.0, 10% glycerol (v/v), 0.9% βOG (w/v). The column was washed with the same buffer plus 10 mM imidazole. The protein was eluted by a linear gradient of imidazole (10 to 400 mM).

The fractions containing the OprM protein, eluted between 100 to 250 mM imidazole, were concentrated up to 5 mg/ml by a 30 kDa cutoff Amicon system (Millipore) and its buffer changed for the following storage solution, 50 mM sodium phosphate, 100 mM NaCl, 10% Glycerol and 0.9% detergent pH 7.5.

2.4. Lipid Bilayer Formation

Firstly, 38 μL of buffer solution was introduced in the upper chamber, and 8 μL of lipid solution followed by 38 μL of buffer solution was flowed into the bottom channel. A layer of lipid membrane formed over the aperture in the parylene film.[12,17,18] Then, the two electrodes were inserted respectively in the chamber and fluidic channel inlet (Fig. 2). 2 μL of 5 μg/mL OprM solution was then added into the upper recording chamber, leading to a final protein concentration of 1.5 nM.

2.5. Optical and Electrical Monitoring

The above-mentioned procedure was performed on an inverted optical microscopy stage (ECLIPSE T*i*-S, NIKON, Japan) covered by a Faraday cage to protect it from the ambient noise. Formation of the BLM was optically monitored from the bottom of the chip with a transmitted light. The membrane current was measured using a patch-clamp amplifier (Axon Axopatch 200B, Molecular Devices, USA) connected to a couple of Ag/AgCl electrodes; one electrode was inserted in the upper recording chamber (*CIS* side, recording electrode), the other was inserted into the bottom channel (*TRANS* side, counter/reference electrode). The Amplifier was connected with a digital data acquisition system (Digidata 1440A and Axopatch 200B, Molecular Devices, U.S.A.).

3. Results and Discussion

3.1. Optical and Electrical Monitoring of Bilayer Lipid Membrane (BLM)

BLM is formed in the chamber, over the 45 μm sized aperture micromachined in the parylene film. After the microfluidic procedure, the circular border separating the BLM, (Fig. 3, central circle) and a supporting annulus (the Plateau-Gibbs border,[19,20] consisting of lipid solution contained between two phospholipids monolayers) appeared spontaneously within 10 min in the aperture. Using this method, the BLM can be achieved easily with a success rate

higher than 90% (calculated from more than 220 experiments out of 50 chips). As reported before, this Plateau-Gibbs border was no longer visible if the aperture in the parylene partition becomes smaller than 45 µm, which is probably due to the optical diffraction.[12] BLM formation was visualized through phase contrast microscopy. As shown on Fig. 3 the size of the reconstructed BLM depends directly on the applied voltage between *CIS* and *TRANS* sides. The electric capacitance of the BLM was measured by applying square signals across the membrane using a built-in function of Clamplex V10.2 software. A rapid increase in electric capacitance was observed upon the BLM formation, and the specific capacitance (Cs, capacitance over the total area of BLM) reached 0.58 µF/cm^2. This value is higher than the Cs of BLM formed with n-decane reported in the literature (~0.4 µF/cm^2) because mixture solvent of 1-Hexanol (80%) and n-Decane (20%) was used to achieve BLM.[20] This phenomenon is consistent with previous observations.[14] we compensated the evaporation by adding some buffer to the chamber and channel thanks to the access to the both sides of BLM within the device.

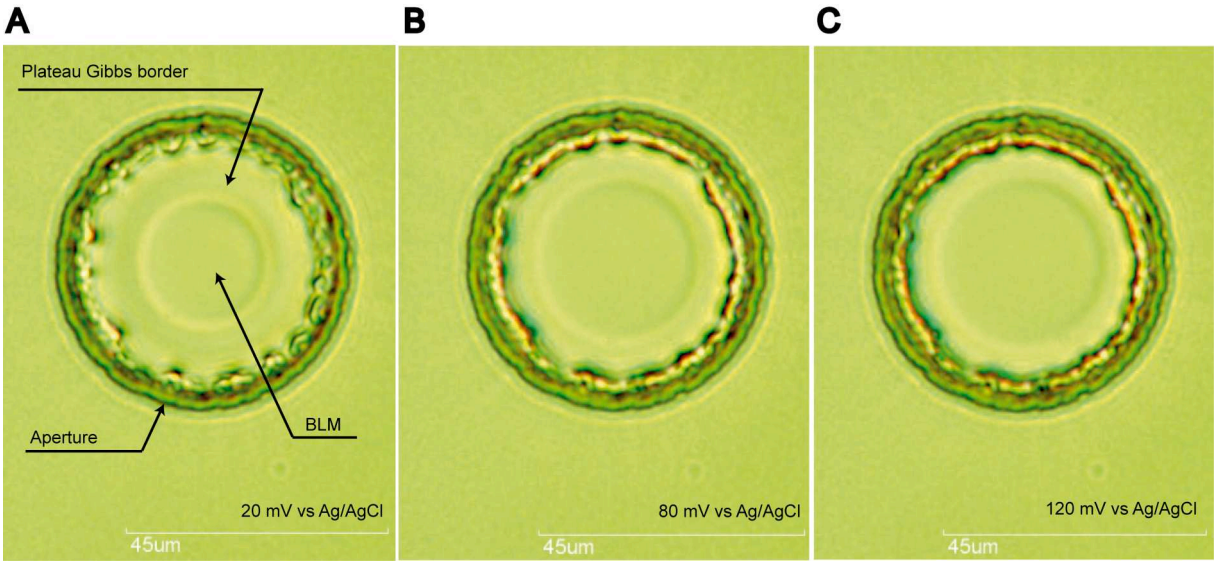

Fig. 3 The typical bilayer lipid membrane (BLM) reconstituted in the parylene aperture. The 45 µm diameter aperture in the parylene film (dark circle) contains the BLM (central circle) which is supported by the thick lipid plateau-Gibbs border. The voltage applied between both sides of the BLM

affects its size: the BLM diameter increases from 20 µm (4A) to 40 µm (4C) while the transmembrane voltage increases from 20 mV to 120 mV. This dependence is explained by static charges stored between both sides of the membrane (Q=CV, where C is the capacitance of the BLM and V the applied voltage) which attract each other, and repeals the solvent towards the border of the aperture in the parylene film. Lipid solution: 25 mg/ml DPhPC in mixture solvent (80% 1-Hexanol and 20% n-Decane, v/v), buffer: 50 mM KCl + 100 mM NaCl + 0.45% (w/v) βOG, pH = 7.5.

3.2. Electrical Recording of OprM Reconstituted in the Membrane

The OprM protein solution was added from either the channel or chamber sides. Both cases permitted successful OprM insertion and activity monitoring. The electric potential is always given at *CIS* side with respect to the *TRANS* side. This electrical potential must be negative for OprM insertion from the micro channel, or positive if OprM is injected in the micro chamber. The insertion events appear several minutes after OprM injection, once the BLM and fluids in the micro channel are stable (typically at t = 5 min). During this stabilization process, the clamp voltage was progressively increased and the conductance of the membrane was monitored. Single ion channel insertion and activities were recorded.

Case of OprM injected in the micro-channel: 38 µL of 1.5 nM OprM solution was flowed in the channel, and negative potential was applied in the chamber. Ion channel was reconstituted into the BLM, which was accompanied by a fast increase of conductance (Fig. 4, G_i = 1250 pS).

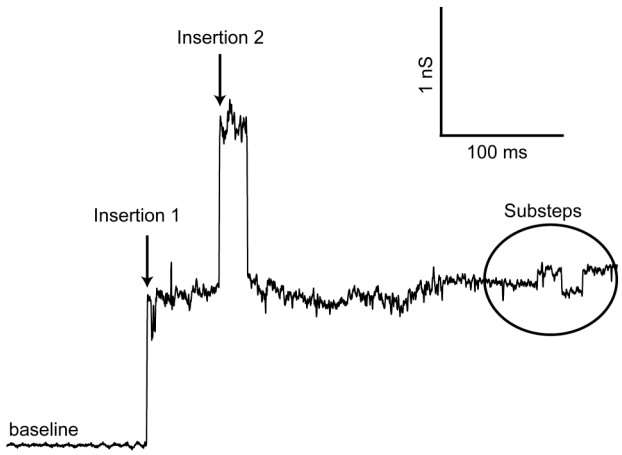

Fig. 4 Channel side insertion. Electrical monitoring of OprM insertion and its activity. OprM was loaded from the micro-channel. A fast rise of conductance G_i = 1250 pS occurs during the insertion event at an applied voltage -120 mV. Buffer: 50 mM sodium phosphate + 100 mM sodium chloride + 0.45% (w/v) βOG, pH = 7.5, Lipid: 25 mg/ml DPhPC in mixture solvent (80% 1-Hexanol and 20% n-Decane, v/v). Recording conditions: filter low pass 10 kHz, sampling 50 kHz. Boxcar smoothing, 27 points.

Case of OprM injected in the micro-chamber: When OprM was added from the chamber side, 2 µl of 30 nM OprM was injected into the buffer from chamber after the BLM was formed and stable. A positive potential was applied in the chamber. Ion channel were also recorded in this case characterized by a fast increase of the conductance (Fig. 5, G_i = 1250 pS).

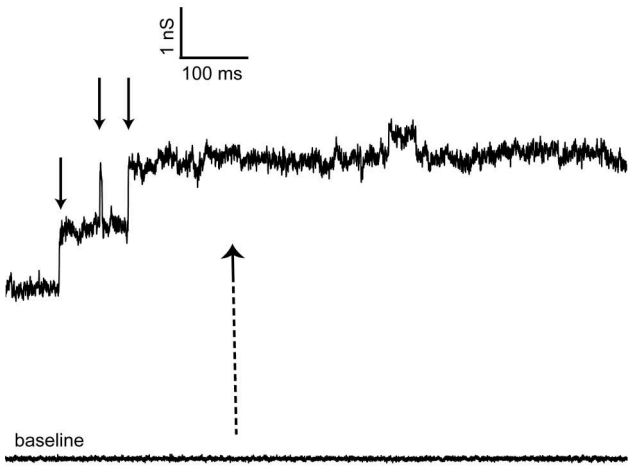

Fig. 5. Chamber side insertion**.** Electrical monitoring of OprM insertions (each insertion event is indicated with a solid line arrow). Fast rise of conductance G_i = 1250 pS occurs for each insertion event at an applied voltage of 50 mV. Buffer: 50 mM sodium phosphate + 100 mM sodium chloride + 0.45% (w/v) βOG, pH = 7.5, Lipid: 50 mg/ml PC in n-Decane). Recording conditions: filter low pass 2 kHz, sampling 10 kHz. Boxcar smoothing, 5 points.

Hence, it appears that the conductance steps are similar when the protein is inserted from either side of the bilayer (Fig. 4 and 5). Note that inserting from the chamber side appears to be more relevant because it makes possible to add the protein several times, as its activity declined with time, without perturbing the stability of the BLM. The activity of OprM depends mainly on the preparation process, the storage and unfreezing conditions. According to our experimental observations, the OprM activity declines after 30-60 min once inserted, and the BLM can be stable for more than 1 h electrical recording.

Fig. 4 and 5 (corresponding respectively to channel and chamber insertion) show the typical step-like increases in trans-membrane current that characterize the successive single OprM channel insertions, with 1250 ± 13 pS (mean ± standard error calculated on 200 events) increase in conductance for each single insertion (see the solid line arrows). The measured single channel conductance of OprM stays comparable over 200 insertion events (1250 ± 13 pS), which indicates the successful and reproducible insertion of native OprM.

3.3. Influence of the buffer composition on conductance

As reported, OprM channel is cation selective.[21] New experiments were designed to study the effects of buffer composition on conductance by monitoring the conductance of OprM in 150 mM K^+ medium instead of 150 mM Na^+ medium. The results show a significant decrease in single OprM channel conductance from 1250 ± 13 pS in the presence of 150 mM Na^+ to 380 ± 5 pS in the presence of 150 mM K^+. When increasing the concentration of K^+ from 150 mM

to 1 M, the conductance increased from 380 ± 5 pS to 726 ± 36 pS. The use of K^+ instead of Na^+ strongly decreases the conductance of a single OprM channel.

These measurements are consistent with OprM conductance reported (850 pS, versus 726 pS in our case with 1 M KCl buffer).[21]

3.4. Comparison with other porins

Those values are also comparable with conductance measurements performed with other channel proteins. Experiments reported with OmpF,[22] a trimeric influx porin, in 150 mM KCl gave a conductance of 940 pS for the all-open state trimer leading to ≈ 310 pS for one monomer, to be compared with the 380 pS we measured for OprM in similar conditions.

Published values for TolC,[23] presenting similar inner and outer diameters, indicate 80 pS conductance for a single channel that is much lower than in our case. Nevertheless those experiments were performed in different experimental conditions (1 mM Hepes pH 7.5, 1 M KCl) rending difficult the comparison.

3.5. Effect of Electric Field Orientation on OprM Insertion

Interestingly, we found that reversing the polarity of the applied potential tends to inhibit protein insertions, and leads to the progressive expel of inserted proteins out of the BLM. This shows that a positive voltage is necessary to maintain the ion channel inserted from the chamber within the BLM. It can be explained by the structure of OprM. As we know, OprM inserts into BLM with its β-barrel, which only represents a small part (less than one third length) of the protein. In order to achieve a successful and stable insertion, an electric field with defined direction is needed. This phenomenon has not been reported elsewhere, nevertheless, in the case of TolC,[23] it was mentioned that the conductance noise was more prominent at high negative potential than at positive ones. This could reflect of a more difficult ions crossing in the non-natural direction or/and of different repartition of charges inside the channel.

3.6. Protein Activity and Conductance Sublevels

After the equilibration period, we clearly found that sub-states (identified by distinct conductance sublevels) can be recorded once OprM becomes active within the BLM (Fig. 6). These sub-states last for few milliseconds up to hundred of milliseconds, and could be recorded during a long period (typ. 20 min). According to our observations these sub-states indicated at least five distinct levels (three levels are shown on Fig. 6) that might correspond to the different possible structural conformations of the helix bundles "controlling" the opening of the pore. The oscillation of the protein between those different conformations leads to regular steps variation of the conductance (125 pS) after the insertion event.

4. Conclusions

This paper shows the feasibility to use a microfluidic device, incorporated with a miniaturized artificial BLM, for monitoring the insertion and electrical activity of the OprM protein. This biomimetic device is able to define very stable and optimized conditions. As a result, both the insertion and activity of OprM could be monitored during the same recording for the first time. In this work, the transmembrane voltage necessary for the OprM insertion was investigated, which showed the importance of the electric field direction. Furthermore, the single channel conductance of OprM has been characterized. It was clearly found that the conductance of OprM depended on the nature and concentration of the cations contained in the buffer. The effect of sodium and potassium ions on the OprM conductance has been addressed. The single channel conductance of OprM in sodium medium is 3 times higher than that in potassium medium, which indicated the sodium ion selectivity of OprM. During the electrical monitor of OprM, high-dynamic sub-step activities of OprM were recorded for the first time, which characterized oscillation of the protein between various sublevels, probably corresponding to different arrangements of bundles controlling the conductance of the pore. This work provide

an analysis method in membrane protein investigation and it showes a wide range of potential applications in pharmacology and biochemistry.

Acknowledgments

This work was financially supported by le Centre National de la Recherche Scientifique (CNRS), L'Agence Nationale de la Recherche ANR-PNano and Japan Science and Technology Agency (JST). L. M. was supported by a grant of Vaincre la Mucoviscidose.

REFERENCES

1 T. Strateva and D. J. Yordanov, *Med. Microbiol.*, 2009, **58**, 1133-1148.

2 T. J. Schirmer, *Struct. Biol.*, 1998, **121**, 101-109.

3 R. Koebnik, K. P. Locher and P. Van Gelder, *Mol. Microbiol.*, 2000, **37**, 239-253.

4 H. Nikaido, *Science*, 1994, **264**, 382-388.

5 H. Akama, M. Kanemaki, M. Yoshimura, T. Tsukihara, T. Kashiwagi, H. Yoneyama, S. Narita, A. Nakagawa and T. J. Nakae, *J. Biol. Chem.*, 2004. **279**, 52816-52819.

6 G. Phan, H. Benabdelhak, M. B. Lascombe, P. Benas, S. Rety, M. Picard, A. Ducruix, C. Etchebest and I. Broutin, *Structure*, 2010, **18**, 507-517.

7 V. Koronakis, *FEBS lett.*, 2003. **555**, 66-71.

8 W. F. Wonderlin, A. Finkel and R. J. French, *Biophys. J.*, 1990, **58**, 289-297.

9 N. Fertig, C. Meyer, R. H. Blick, C. Trautmann and J. C. Behrends, *Phys. Rev. E. Stat. Nonlin. Soft. Matter. Phys.*, 2001, **64**, 040901.

10 B. Zhang, J. Galusha, P. G. Shiozawa, G. Wang, A. J. Bergren, R. M. Jones, R. J. White, E. N. Ervin, C. C. Cauley and H. S. White, 2007. *Anal. Chem.*, **79**, 4778-4787.

11 T. Ide, T. Kobayashi and M. Hirano, *Anal. Chem.*, 2008, **80**, 7792-7795.

12 B. Le Pioufle, H. Suzuki, K. Tabata, H. Noji and S. Takeuchi, *Anal. Chem.*, 2008, **80**, 328-332.

13 M. Kitta, H. Tanaka and T. Kawai, *Biosens. Bioelectron.*, 2009, **25**, 931-934.

14 T. Osaki, H. Suzuki, B. Le Pioufle and S. Takeuchi, *Anal. Chem.*, 2009, **81**, 9866-9870.

15 N. Fertig, M. George, M. Klau, C. Meyer, A. Tilke, C. Sobotta, R. H. Blick and J. C. Behrends, *Receptor. Channel.*, 2003, **9**, 29-40.

16 R. Kawano, T. Osaki, H. Sasaki and S. Takeuchi, *Small*, 2010, **6**, 2100-2104.

17 H. Suzuki, K. Tabata, Y. Kato-Yamada, H. Noji and S. Takeuchi, *Lab. Chip.*, 2004, **4**, 502-505.

18 H. Suzuki, K. V. Tabata, H. Noji and S. Takeuchi, *Langmuir*, 2006, **22**, 1937-1942.

19 H. S. White, In: Miller, C. (Ed.)*, Ion channels reconstitution. Plenum Press, New York*, 1986, pp. 3-32.

20 H. Fujiwara, M. Fujihara and T. Ishiwata, *J. chem. Phys.*, 2003, **119**, 6768-6775.

21 K. K. Y. Wong, F. S. L. Brinkman, R. S. Benz and R. E. W. Hancock, *J. Bacteriol.*, 2001, **183**, 367-374.

22 A. Baslé, R. Iyer and A. H. Delcour, *BBA-Biomembranes*, 2004, **1664**, 100-107.

23 C. Andersen, C. Hughes and V. Koronakis, *J. Membr. Biol.*, 2002, **185**, 83-92.